

THERMODYNAMICS AND KINETIC STUDY OF EOSIN DYE ADSORPTION ON CuO NANOPARTICLES

Amir. Fahdi Dawood AL-Niaimi¹, Ghalib I Atiya² and Donia A Abdulateef³

^{1,3}Department of Chemistry, College of Science,
Diyala University, Baguba, Diyala, Iraq.

²Department of Chemistry-College of Education for
Pure Science- Diyala University, Iraq.

ABSTRACT

In this study, nanoparticles copper oxide (CuO) was used as adsorbent to the remove Eosin dye from aqueous solution in batch method. The prepared CuO nanoparticles was characterized using X-ray diffraction (XRD), Scanning electron microscopy (SEM), Atomic force microscope (AFM), Fourier transform infrared (FTIR) and Brunauer, Emmett and Teller (BET). Adsorption parameters such as contact time, adsorbent dose, dye concentration, pH, and temperature were studied. Adsorption isotherms been used to test the adsorption data (Langmuir, Freundlich, Dubinin, Temkin) as it was fit to Dubinin-Kaganer-Radushkevich isotherm. Thermodynamic parameters (ΔH° , ΔG° , ΔS°) of adsorption were calculated, which show the adsorption exothermic process and this process followed physisorption mechanism. Kinetic data were fit to pseudo- second order model.

Keywords: Adsorption, Eosin dye, Thermodynamic study and Kinetic study.

INTRODUCTION

Dyes are widely used in industries including textile, printing, plastic, pharmaceutical, leather, paper and a food processing^{1,2}. These industries emits amounts of dye wastes caused water pollution by dyes has become a environmental issue because most of their toxicity to human health and aquatic plant and animal life^{3,4}. Most dyes are stable to light and oxidizing agents and non-biodegradable in nature⁵. Various methods such as reverse osmosis, ion exchange, chemical oxidation, filtration, coagulation, flocculation^{6,7} and adsorption have been applied to remove dyes from aqueous solutions which will be mentioned later, adsorption is easy, safe and effective in water treatment using activated carbon, agricultural residues^{8,9}, graphene oxide^{10,11} etc. The most widespread because carbon has a high porosity¹². The main objective of this work was to investigate the adsorption of eosin dye from its aqueous solutions by CuO.

MATERIALS AND METHODS

Instruments

UV-Visible (Shimadzu, Japan 1700) was used to analyze the dye concentration in aqueous

solution. The pH of all solutions was recorded by pH meter (7110(wtw), Germany). The temperature was controlled using isothermal water bath shaker (BS-11, Korea). CuO characterized using XRD (Shimadzu company (Japan) (XRD-6000)) with Cu α radiation ($\lambda = 0.15406\text{nm}$), the measurements conditions of XRD are 40kv, 30mA, the scanning range is 20-80° and the scanning speed 5 deg/min., FTIR (Shimadzu (IR PRESTIGE 21) with KBr pellet technique. The effective range was from 4000 to 400 cm^{-1} , AFM (SPM-AA3000, Advanced Angstrom Inc.), SEM (Type Tescan), BET (Q-surf 9600 (USA)).

Preparation copper oxide nanoparticles

copper oxide (CuO) nanoparticles was prepared by precipitation method. The copper nitrate solution ($\text{Cu}(\text{NO}_3)_2 \cdot 6\text{H}_2\text{O}$) (0.2 M) was placed in (2000 ml) beaker placed on a hot plate magnetic stirrer. A magnetic bar is used in order to obtain homogeneous mixing of the material. Measure and monitor the pH value of the solution during the slowly addition of the sodium bicarbonate solution (NaHCO_3) (0.4 M) from burette. The temperature of the solution was fixed at 80°C. The addition continued until the pH of the solution reaches (6.8) where the

precipitation was completed. After the completion of reaction, the precipitate is allowed to settle overnight. It is then filtered off and the precipitate is washed several times with distilled water, until free from excess bicarbonate which may be present then dried the precipitates at 70-80 °C for 2 hour and then calcined at 400 °C for 3 hours in an oven to obtain the CuO.

Preparation of Standard Solutions for Eosin dye

A stock solution of the dye with a concentration of (250 ppm) was prepared by dissolving (0.025g) in volumetric flask (1000 ml) of distilled water. Solutions of different concentrations (2 - 20) ppm were prepared by dilutions from the stock solution and left for 24 hours in order to homogenize. (0.1 M) HCl and (0.1 M) NaOH was used for pH adjustment. The UV-Visible spectrometer (Shimadzu U.V-visible, Japan.1700) used to determination calibration curve for eosin dye at λ_{max} (516nm). The dye adsorption by batch process to study different parameter such as contact time (10-100) min ,dose of adsorbate (CuO) (0.01-0.09g), pH(1-10),temperature (20-40°C).The solutions were shaken and kept in a thermostat for (50) min ,the samples were then filtered in a centrifuge for 15 min (at 3500 rpm) and then filtered again and analyzed spectrophotometrically. The percentage dye adsorption from the aqueous solution was determined according to the following equation¹³:

$$\% \text{ Adsorption} = \frac{C_0 - C_t}{C_0} \times 100 \quad (1)$$

Where C_0 and C_e (mg/L), are the initial concentration and the concentration at any time respectively. The adsorption capacity Q_e (mg/g).

$$Q_e = \frac{C_0 - C_e}{m} \cdot V_{sol} \quad (2)$$

Q_e : Amount of solute adsorbed per unit weight of adsorbent (mg/g).

C_e : Equilibrium concentration of solute (mg/L). V_{sol} : Volume of solution (L). m : Mass of adsorbent(g).

RESULTS AND DISCUSSION

Characterization of CuO Nanoparticles

Figure (1) show the FTIR spectra of CuO nanoparticles has a noticeable peak at 540 and 560 cm^{-1} which are attributable to Cu-O stretching modes, confirming the formation of highly pure CuO nanoparticles a band at 669 cm^{-1} was attributed to Cu_2O . The sample have

the absorption peaks in the range of 1637-1445 cm^{-1} that may be assigned to O-H bending vibrations combined with copper atoms¹⁴.

In Figure (2) the crystal planes of (110), (002) and (111) belong to monoclinic system. All data in good agreement with JCPDS files **NO. 45-0937**, cell parameter ($a = 4,685$, $b = 3.425$, $c = 5.130$ Å) and no other phases are detected, and the diffraction peaks are sharp with the crystal growing completely with high purity. Figure (2) show the XRD pattern of CuO nanoparticles sample. It is very clear that the major reflections between ($2\theta = 30^\circ - 40^\circ$) indicate more crystalline regions in the CuO sample. The detailed analysis of the XRD and the assignments of various reflections are given in the Table (1). Particle size has been estimated by using Debye-Scherrer's Equation(3).

$$D = 0.9\lambda / \beta \cos \Theta \quad (3)$$

Where D: crystallite size, λ wave length (0.154nm), β : full width at half maximum, Θ : diffraction angle, $D = 23.4$ nm calcined at 400 °C¹⁵.

The specific surface area of adsorbents surfaces should be determined if any physical chemical interpretation of its behavior as an adsorbent is to be possible. The properties of surface area were provided through the adsorption of nitrogen at 77 K which is the temperature equilibrium between the vapor and liquid phase. The results of surface area for the (CuO) nanoparticles are 35.6351 m^2/g . The SEM images of the CuO nanoparticles sample that prepare by precipitation method are shown in Figure (3), a homogeneous distribution of spherical shape and with irregular distribution. From SEM images it is confirmed that the particles having size (39-41) nm.

Atomic force microscopy (AFM) is a powerful characterization tool for determination the particle size and surface organization of the synthesized materials. The wet ability of a surface is dependent on its chemical composition, and also on the topography of the surfaces. (CuO) nanoparticles are characterized by AFM image in two and three-dimensional and particles sizes distributions for adsorbent surface was represented in Figures (4, 5). They show that the average diameter of the particle CuO was (39.4 nm)¹⁶.

Determination of Equilibrium Time of adsorption

Several adsorption experiments in (10-100) min of contact time range were performed and the results were shown in Fig.6. The removal

rate of dye onto CuO gradually increased with the increase of contact time from 10 to 50 min and then remained constant¹⁷, with further increase in contact time; therefore, a period of 50 min of equilibrium was selected for the next studies. In the initial stage, dye contact quickly with a lot of available active sites on the surface of CuO, resulting in the occurrence of the fast adsorption with increase of the contact time, the available active sites gradually lessened and the driving force weakened, leading to the slow adsorption process and taking long time to achieve adsorption equilibrium.

Adsorbent Weight

The effect of adsorbent on percentage removal of dye was examined by taking different quantities of CuO ranging from 0.01 to 0.09 gm. Our results showed in Figure (7), that the best removal efficiency was obtained at 0.04gm. The number of a site available for adsorption site increases by increasing the adsorbent weight, but as the time passes, active sites become saturated and thus slowing down the removal of dye¹⁸.

Effect the concentration of dye on adsorption

Figure (8) shows that the effect concentration of dye on percentage removal of dye by taking different quantities of dye ranging from 2 to 20 ppm. Our results showed the best removal efficiency was obtained at 10 ppm.

Effect of pH

The initial pH of the eosin dye solution can significantly affect the adsorption capacity of the dye because it affects the charge distribution of the surface of the adsorbent (CuO) as well as adsorbate (the dye molecules). The effect of pH was studied by changing pH(4,7,and 10) and with different concentrations of dye (2-20)ppm. Figure (9) shows that in acidic medium the adsorption capacity is maximum and decreases with the increase pH and according to the following pH = 4 > 7 > 9. To the study of better pH for the adsorption of Eosin dye through the preparation of ten volumetric flasks (50 ml) containing equal volumes (30 ml) of initial concentration (18) ppm with weight (0.04 g) for (CuO) nanoparticles and with change the pH (1-10) for each flask at 25 °C, the results interactions between adsorbed ions ,atoms or molecules²¹. With each molecule adsorbed onto the surface having the same adsorption energy .The Langmuir isotherm²² is expressed as:

shown in Figure (10).

Adsorption Kinetics studies

In order to assess the rate of the adsorption for eosin dye, both pseudo first order and pseudo second order kinetics were applied to the adsorption data¹⁹.

$$\ln (q_e - q_t) = \ln q_e - k_1 t \quad (4)$$

$$t / q_t = 1 / k_2 q_e^2 + (1 / q_e)t \quad (5)$$

Where q_e and q_t (mg/g) are the amounts of dye adsorbed at equilibrium and time t respectively, k_1 and k_2 are the rate constant of pseudo first order (min^{-1}) and pseudo second order ($\text{g/mg} \cdot \text{min}$).The plots of the equations were examined for best fit by comparing their correlation coefficients (R^2). Figure (11 and 12) shown the straight plots of $\ln (q_e - q_t)$ vs t and t / q_t vs t , respectively. The correlation coefficients of the linear curves of both kinetics shows that the process more likely follows a second order kinetics. Pseudo-second order model assumes that the rate –limiting step involves chemisorption of adsorbate on the adsorbent. By fitting the experimental data (Figures 11and 12), the adsorption rate constant for each model was calculated and summarized in Table (2). The kinetics data were well fitted by the pseudo-second order, as demonstrated by the higher regression coefficient (R^2) obtained .In addition, the calculated q_e values for the pseudo-second order is highly matched with the experimental data as compared with those of the pseudo-first order model. This indicated that the adsorption kinetics of dye on CuO was not diffusion controlled²⁰.

Adsorption isotherm studies

The adsorption isotherms are to explore the relation between the adsorbate concentration in the bulk (at equilibrium) and the amount adsorbed at the surface. In this study four commonly used isotherm models (Langmuir, Freundlich, Temkin, and Dubinin-Kaganer-Radushkevich) were applied to the experimental data to explain the dye –CuO interaction. The Langmuir isotherm model assume monolayer coverage of the adsorbate over a homogenous adsorbent surface with identical adsorptions sites and their binding energies and neglecting any

$$\frac{C_e}{Q_e} = \frac{1}{q_{\max} k_L} + \frac{C_e}{q_{\max}} \quad (6)$$

Where C_e is the equilibrium concentration of dye (mg/L), q_{\max} , Q_e are the maximum adsorption capacity corresponding to complete monolayer coverage on the surface (mg/g)

and capacity at equilibrium (mg/g) respectively and K_L is Langmuir constant (L/mg)²³. related to energy of sorption. Therefore, a plot of C_e/Q_e versus C_e gives a straight line of slope $1/q_{max}$ and intercept $(1/ K_L q_{max})$ from the intercept and slope of the plots in Figure (13). The values of q_{max} and K_L were listed in Table (4). Table (4) shows that the values of q_{max} and K_L are increased when the solution temperature increased from 20 to 40°C, indicates that the dye is favorably adsorbed by CuO at lower temperatures, which shows that the adsorption process is endothermic. A dimensionless constant separation factor of Langmuir isotherm (R_L) was also calculated²⁴ using equation 7:

$$R_L = 1 / (1 + K_L C_o) \quad (7)$$

C_o is the initial concentration of Eosin dye solution (mg/L) and K_L (L/mg) is the Langmuir adsorption constant given in Table (3). Table (3) explains the relation between R_L and the nature of adsorption.

The Freundlich model is a case for multilayer adsorption and adsorption on heterogeneous surface energies and it gives an exponential distribution of active sites. The linear form of this model is represented by:

$$\ln Q_e = \ln K_F + 1/n \ln C_e \quad (8)$$

The Freundlich constants K_F and n , which respectively indicating the adsorption capacity and the adsorption intensity, are calculated from the intercept and slope of plot $\ln Q_e$ versus $\ln C_e$ respectively, as shown in Figure (14). The intensity of adsorption (n) showed low values ($n < 1$); this indicates a very low affinity between adsorbents and adsorbate. The Freundlich constant (K_F) decreases with increasing the temperature and this indication for exothermic reaction. The values of n are larger than (1), which represents a favorable removal condition²⁵.

A more common isotherm than Langmuir is the Dubinin-Kaganer –Radushkevich (DKR) model was proposed by Dubinin which does not assume a homogenous surface of surface of sorbent. It is applied to determine the adsorption mechanism (physical or chemical). The linear form of (DKR) as follows²⁶:

$$\ln Q_e = \ln q_{max} - \beta \epsilon^2 \quad (9)$$

Where q_{max} is the maximum sorption capacity (mg/g), β is the activity coefficient related to

mean sorption energy (mol^2/J^2), and ϵ is the Polanyi potential defined as:

$$\epsilon = RT \ln (1 + 1/C_e) \quad (10)$$

Where R is the gas constant (KJ/mol. K). The slope of the plot of $\ln q_e$ versus ϵ^2 gives β and the intercept yields the sorption capacity q_{max} , as shown in Figure (15). Prognostication of the adsorption mechanism (physical or chemical sorption) can be done by calculating the value of the mean sorption energy, E (J/mol) from the relation²⁷:

$$E = (-2 \beta)^{-0.5} \quad (11)$$

The values of β , q_{max} , E and R^2 as a function of temperature are listed in Table (4). If the values of E were less than 8 kJ/mol, the mechanism maybe a physical adsorption, While E values between 8-16 kJ/mol assumes the adsorption to be controlled by ion exchange and E greater than 16 kJ/mol presume a particle diffusion mechanism (chemical process). It can be observed that the values of E may be physical (electrostatic) in nature.

The Temkin isotherm in the linear form has been used as the following:

$$Q_e = B \ln K_T + B \ln C_e \quad (12)$$

Where $B = RT/b$ is related to heat of adsorption of adsorption (J/mol), K_T is equilibrium binding constant (L/gm), R is the gas constant (8.314 J/mol. K). Both K_T and B are calculated (as shown in Table (5)) from the intercept and the slope of curve between $\ln C_e$ and Q_e as in Figure (16).

As presented in Table (4), the adsorption of Eosin dye on CuO nanoparticles was fit to Dubinin-Kaganer-Radushkevich isotherm by higher correlation factor (R^2) values. The results show what is otherwise based on the correlation coefficient data²⁸.

The values of dimensionless sorption factor (K_L) were close to zero and this indication for favorable adsorption. The intensity of adsorption (n) showed low values ($n < 1$); this indicates a very low affinity between adsorbents and adsorbate. The Freundlich constant (K_F) decreases with increasing the temperature and this indication for exothermic reaction. In isotherm Dubinin (DKR), the energy equation gives us a perception of the adsorption mechanism.

($E < 8$ KJ /mol) indicates that the physical force

influence adsorption and that ($E > 16$) indicates the spread of molecules and when (E) is between (8-16) indicates that adsorption is directed by ion exchange, and the values of (B) less than (40 kJ/mol) this indication for physical adsorption⁹.

Thermodynamics parameters

The thermodynamics parameters (ΔH° , ΔG° , ΔS°) of the removal of dye on ZnO were calculated according to the following relations:

$$K_c = A e^{-\Delta H/RT} \quad (13)$$

$$\ln X_m = -\frac{\Delta H}{RT} + K \quad (14)$$

Where $\ln X_m$ is the natural logarithm for greatest amount adsorbed (mg/g), K is the constant of Van't Hoff equation, R is the universal gas constant ($8.314 \cdot 10^{-3}$ J/mol.K⁻¹) and T is the temperature in Kelvin.

$$\Delta G^\circ = -RT \ln K \quad (15)$$

$$K = \frac{Q_e \times m}{C_e \times V}$$

$$\Delta G^\circ = \Delta H - T \Delta S^\circ \quad (16)$$

$$\Delta S^\circ = \frac{\Delta H - \Delta G^\circ}{T} \quad (17)$$

The value ΔH° was calculated from the slope and intercept of the Van't Hoff plots (the plots of $\ln X_m$ versus $1/T$) (Figure (17)) and listed in Table (5)²⁹. The value of ΔH° was negative, indicating that the sorption reactions is exothermic. The negative value of ΔS°

confirmed the decreased randomness as solid/solution interface during the adsorption process³⁰.

CONCLUSION

Based upon the experimental results of this study show that nano-CuO can be considered as an adsorbent for the treatment of eosin dye from waste water. In batch experimentals, the influence of contact time, initial dye concentration, amount of CuO, temperature were show to be effective. The removal of dye is an exothermic process. It was found that the pseudo –second order model might have followed by the adsorption process as supported by correlation coefficients of the linear plots, and also q_{cal} were very close to the q_{exp} for the pseudo –second order rate kinetics. The isotherm study indicates four isotherms models Adsorption data was fit to Dubinin-Kaganer-Radushkevich isotherm, the Freundlich constant (k_F) decreases with increasing the temperature and this indication for exothermic. In isotherm Dubinin (DKR), the energy equation gives us a perception of the adsorption mechanism. ($E < 8$ KJ /mol) indicates that the physical force influence.

ACKNOWLEDGMENTS

Authors wish to thank department chemistry, College of Education for Pure Science and department chemistry ,college science , Diyala university for providing instrument facilities to carry out the research work.

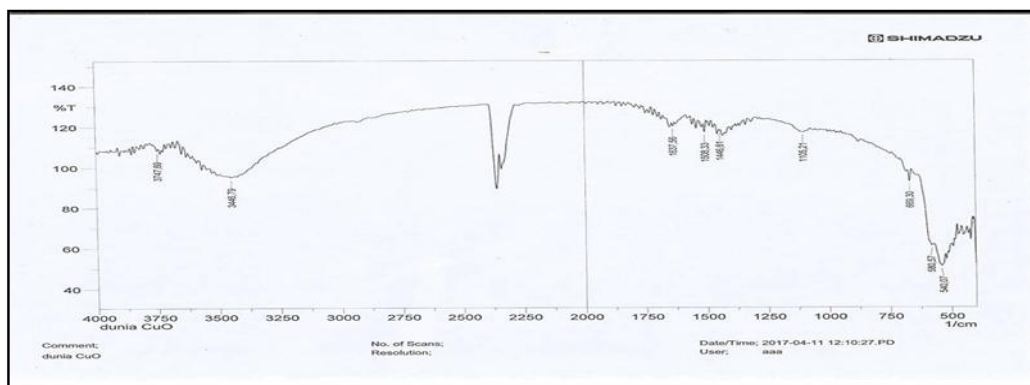


Fig. 1: FTIR spectra of CuO nanoparticles

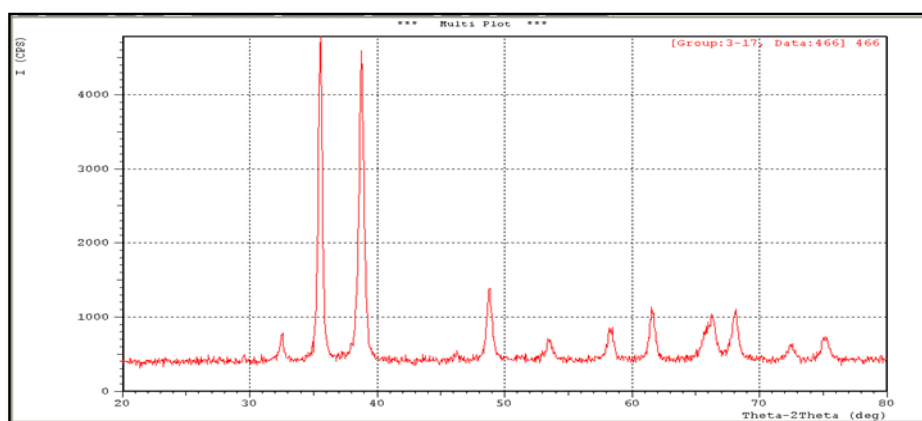


Fig. 2: XRD pattern of CuO nanoparticles

Table 1: Strongest three peaks in XRD of CuO nanoparticles

No	Peak No	(deg) θ 2	d(A)	FWHM (deg)	Intensity Counts
1	2	35.5496	2.52329	0.35890	1748
2	4	38.7735	2.32058	0.43660	1595
3	5	48.7942	1.86487	0.41920	410

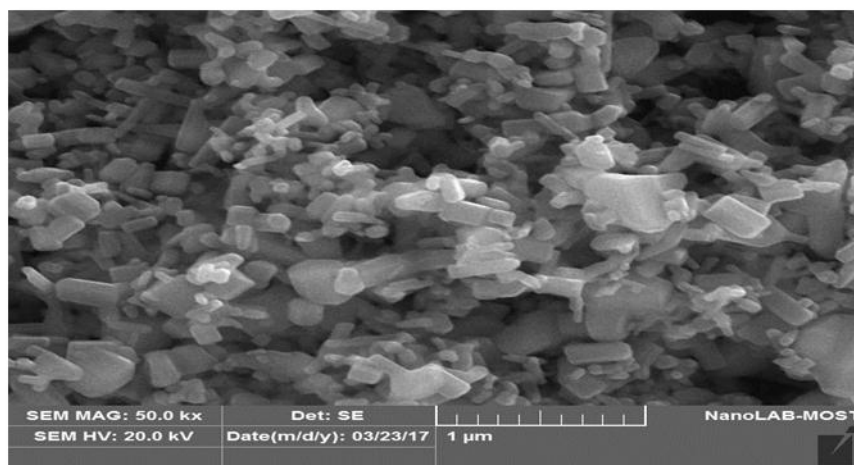


Fig. 3: SEM image of CuO nanoparticles

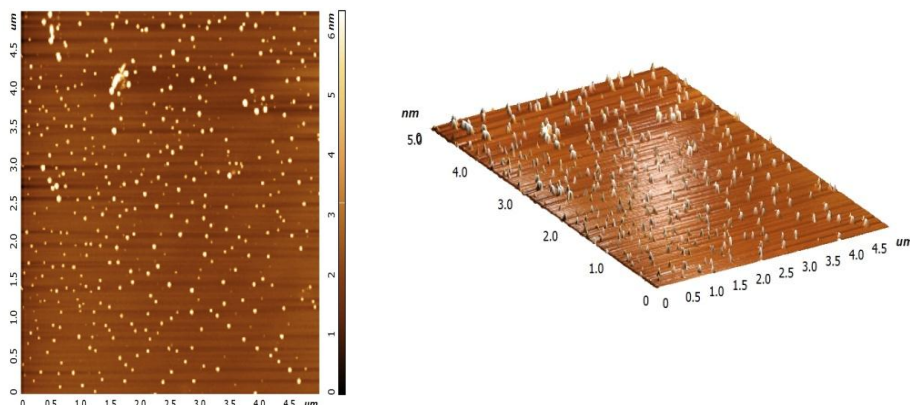


Fig. 4: AFM images of ZnO nanoparticles

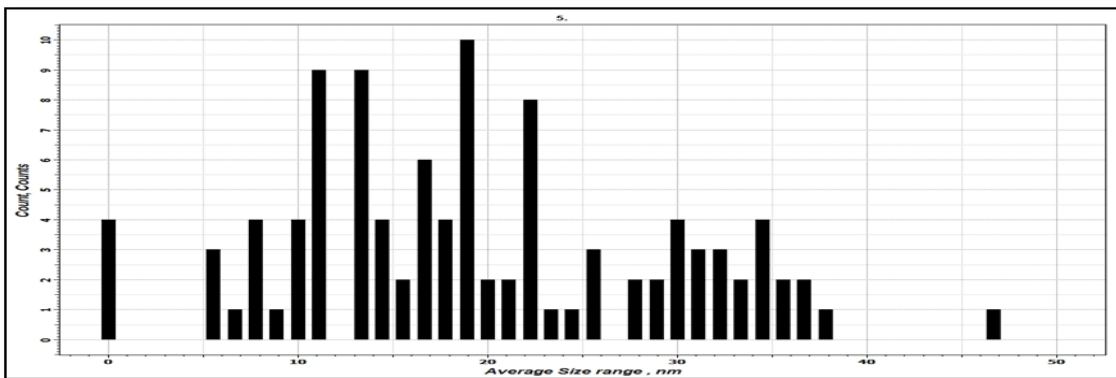


Fig. 5: Particle size distribution of CuO nanoparticles

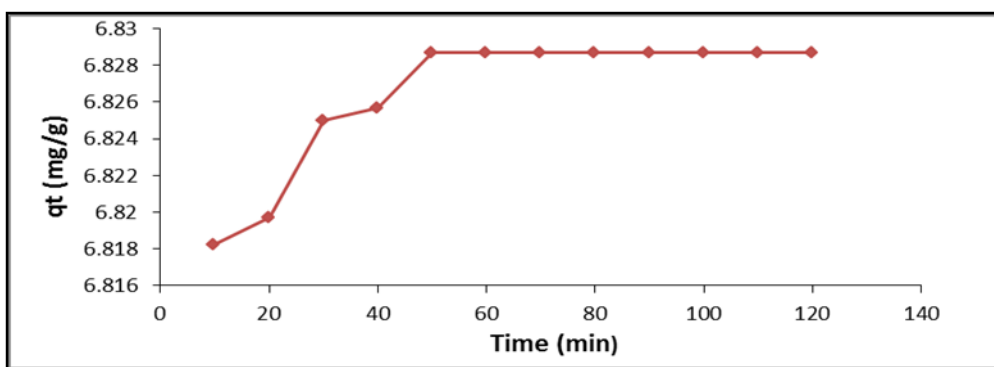


Fig. 6: Effect of equilibrium time for adsorption of Eosin dye on (CuO) nanoparticles (25 °C, Co= 30 ml of 10 ppm, dose 0.04 g and pH=7)

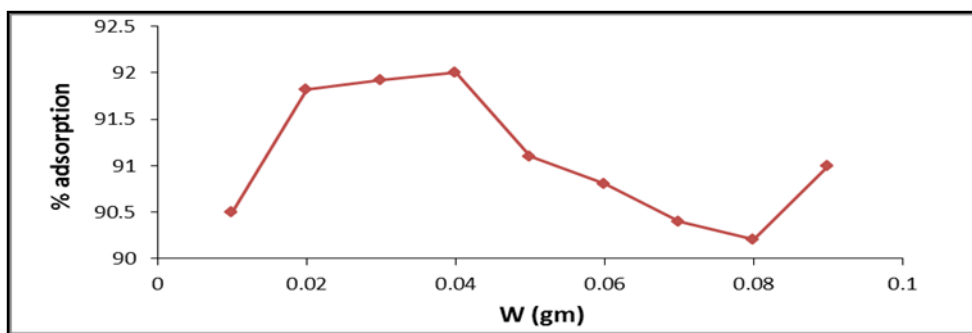


Fig. 7: Effect of adsorbents weight on the adsorption of Eosin dye on (CuO) nanoparticles at (25 °C, C₀=30ml of 10 ppm and pH=7)

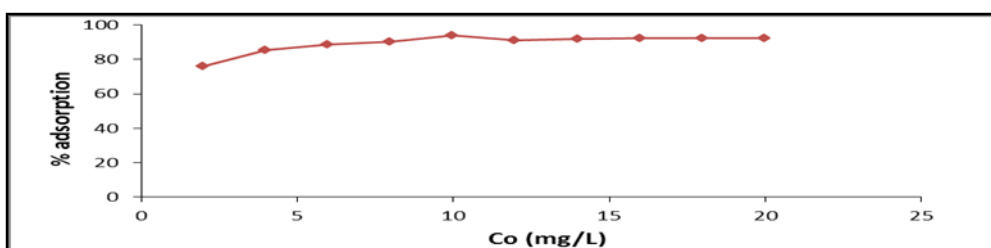


Fig. 8: Effect of dye concentration on adsorption of Eosin dye on (CuO) nanoparticles at 25 °C, dose 0.04gm, pH =7

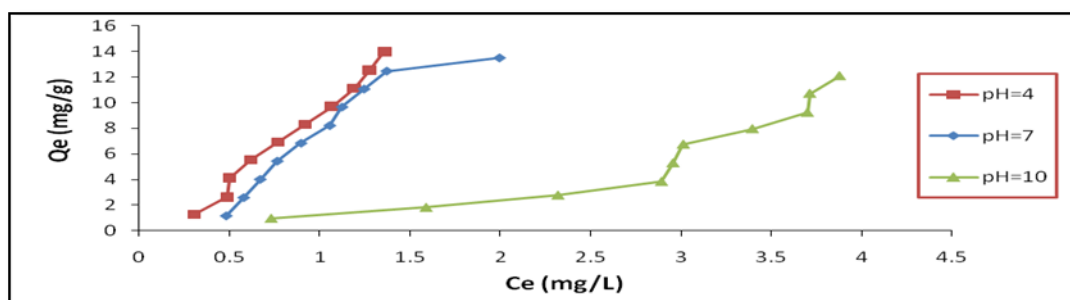


Fig. 9: Effect of pH on the adsorption of Eosin dye on CuO nanoparticles at (25°C, 30ml of 10 ppm dye and dose 0.04gm)

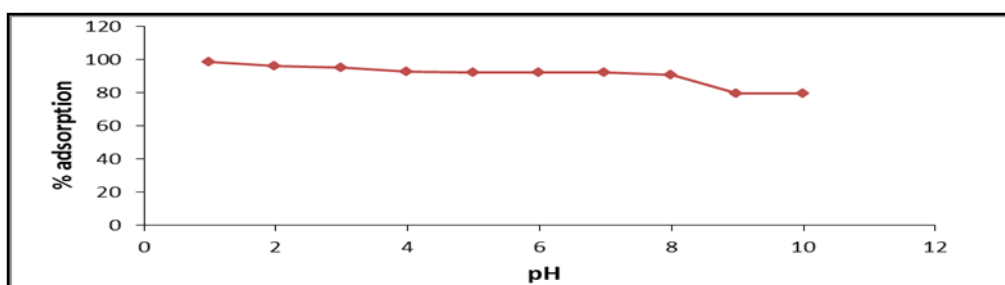


Fig. 10: Effect of pH on the adsorption of Eosin dye on CuO nanoparticles at (25°C, 18 ppm dye and dose 0.04gm)

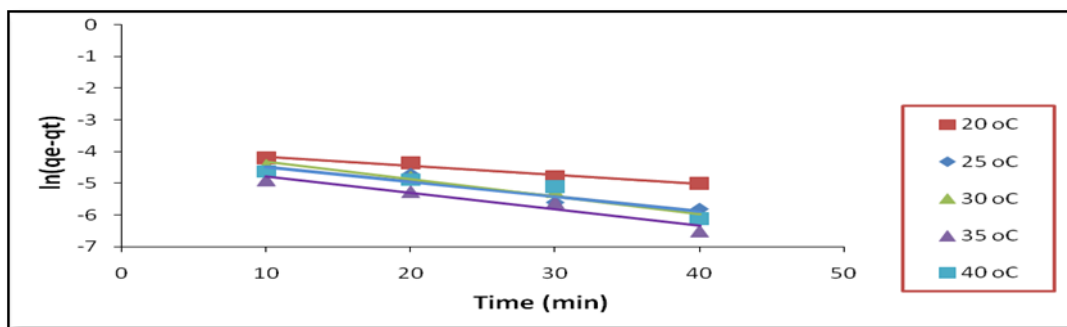


Fig. 11: Plot of pseudo-first order model of Eosin dye on CuO

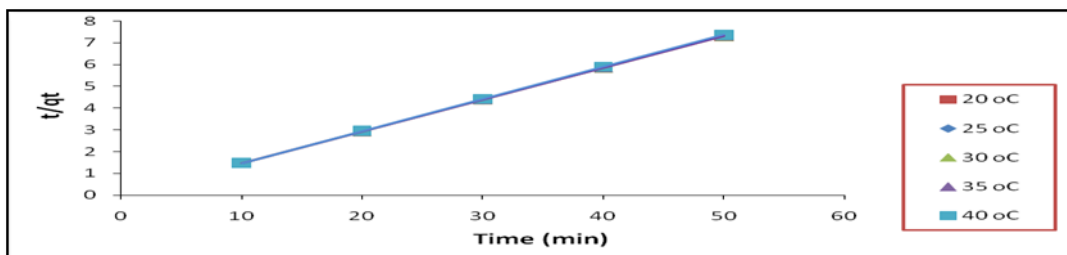


Fig. 12: Plot of pseudo –second order model of eosin dye on CuO

Table 2: Kinetics parameters for adsorption of Eosin dye on CuO nanoparticles

C _o 10ppm	T (°C)	qe(exp)	Pseudo first order			Pseudo second order			
			Qe (calc)	K ₁ min ⁻¹	R ²	q _e (calc)	K ₂ g ⁻¹ .mg.min ⁻¹	H	R ²
	20	6.839	0.020	0.028	0.969	6.839	4.048	189.33	1
	25	6.828	0.018	0.046	0.914	6.830	7.194	335.59	1
	30	6.825	0.023	0.055	0.960	6.825	6.134	285.72	1
	35	6.816	0.013	0.051	0.937	6.816	6.211	288.54	1
	40	6.782	0.017	0.046	0.863	6.784	6.211	285.84	1

Table 3: Values of R_L and type of isotherm

Value of R _L	R _L > 1	R _L = 1	R _L < 1	R _L = 0
Type of isotherm	Unfavorable	Linear	Favorable	eversibleIrr

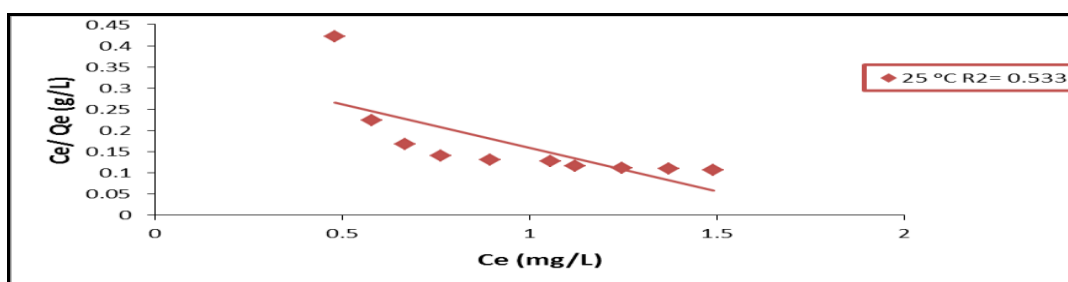


Fig. 13: Isotherm Langmuir for Eosin dyes on CuO nanoparticles at 25 °C

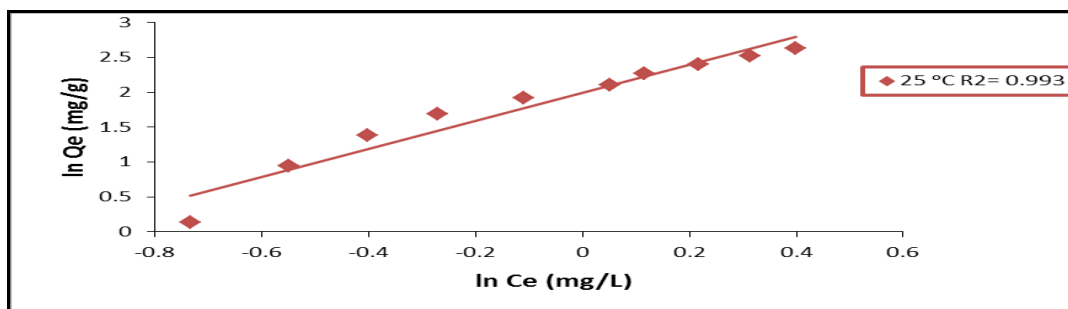


Fig. 14: Isotherm Freundlich for Eosin dyes at 25 °C

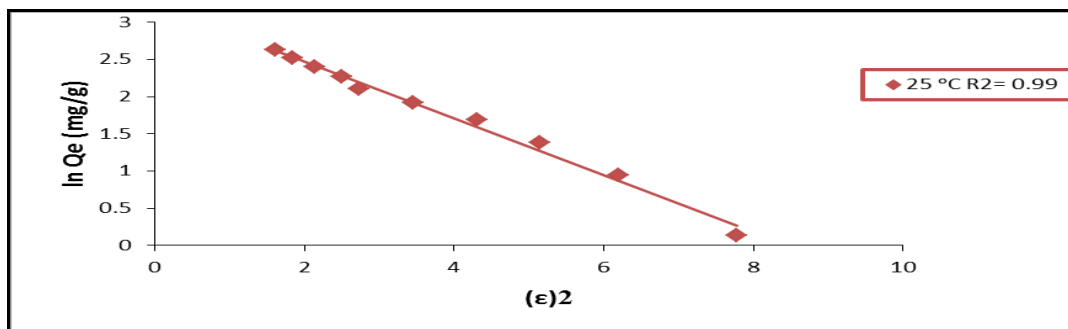


Fig. 15: Isotherm Dubinin (DKR) for Eosin dye at 25 °C

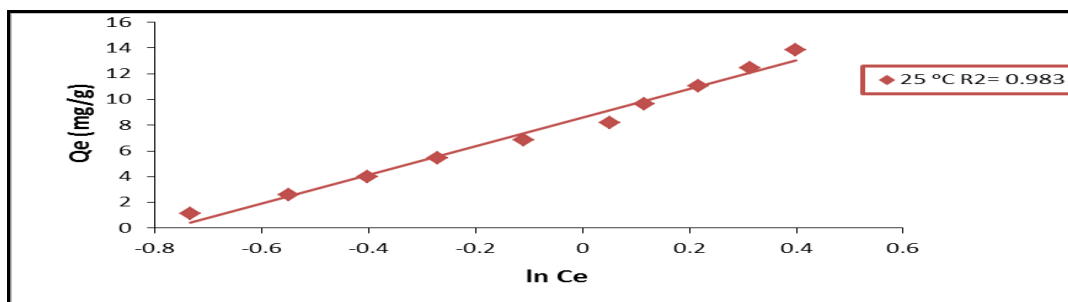


Fig. 16: Isotherm Temkin for Eosin dye at 25 °C

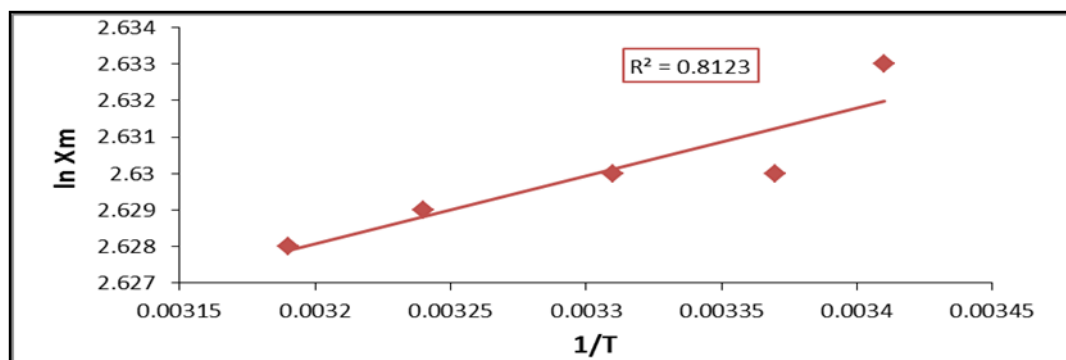
Table 4: The calculated adsorption parameters of the four used isotherms

T(°C)	Langmuir				Freundlich		
	K_L	R^2	q_{max}	R_L	K_F	$1/n$	R^2
20	0.558	0.521	5.216	0.151	7.008	0.457	0.168
25	0.563	0.533	4.889	0.150	7.346	2.007	0.943
30	0.570	0.532	4.766	0.149	5.939	1.178	0.647
35	0.577	0.543	4.595	0.147	6.959	2.051	0.946
40	0.581	0.567	4.492	0.146	6.702	2.062	0.953

(DKR)				Temkin		
β	q_{max}	E	R^2	K_T	B	R^2
-0.3802	25.229	1.146	0.992	17.081	2.988	0.244
-0.3824	25.513	1.143	0.990	2.166	11.123	0.983
-0.3781	25.720	1.149	0.989	3.228	6.337	0.638
-0.3760	25.780	1.153	0.989	2.085	11.290	0.981
-0.3556	25.158	1.185	0.988	2.050	11.246	0.972

Table 5: Values of thermodynamic functions for adsorption Eosin dye on (CuO)

C _e (mg/L)	Thermodynamic function	20 °C	25°C	30 °C	30 °C	40 °C
20 ppm	ΔH KJ.mol ⁻¹	-0.154				
	ΔG KJ.mol ⁻¹	-5.534	-5.529	-5.605	-5.680	-5.826
	ΔS KJ.mol ⁻¹ .k ⁻¹	0.0183	0.0180	0.0179	0.0180	0.0178

**Fig. 17: Values of greatest amounts adsorbed ($\ln X_m$) for Eosin dye on (CuO) nanoparticles at different temperatures (293-318 K)****REFERENCES**

- Arzani Kaveh, Ashtiani BG and Kashi AHA. Equilibrium and Kinetic Adsorption Study of the Removal of Orange-G Dye Using Carbon Mesoporous Material. *Journal of inorganic materials*. 2012;27(6):660-666.
- Li YH, Liu T, Du Q, Sun J, Xia Y, Wang Z and Wu D. Adsorption of cationic red X-GRL from aqueous solutions by graphene: equilibrium, kinetics and thermodynamics study. *Chemical and Biochemical Engineering Quarterly*. 2012;25(4):483-491.
- Kant R. Adsorption of dye eosin from an aqueous solution on two different samples of activated carbon by static batch method. *Journal of Water Resource and Protection*. 2012; 4(02):93.
- Reddy SS, Kotaiah B, Reddy NSP and Velu M. The removal of composite reactive dye from dyeing unit effluent using sewage sludge derived activated carbon. *Turkish Journal of Engineering and Environmental Sciences*. 2007;30(6):367-373.
- Wang L, Zhang J, Zhao R, Li C, Li Y and Zhang C. Adsorption of basic dyes on activated carbon prepared from *Polygonum orientale* Linn: equilibrium, kinetic and thermodynamic studies. *Desalination*. 2010;254(1):68-74.
- Szyguła A, Guibal E, Ruiz M and Sastre AM. The removal of sulphonated azo-dyes by coagulation with chitosan. *Colloids and Surfaces A: Physicochemical and engineering aspects*. 2008; 330(2):219-226.
- Mishra A and Bajpai M. The flocculation performance of Tamarindus mucilage in relation to removal of vat and direct dyes. *Bioresource technology*. 2006;97(8):1055-1059.
- Amir F Dawood and Abd AL-Rahman.K, and Marwa I Mubarak. Study eosin dye adsorption on the surface wheat chaff. *Diyala Journal for Pure Sciences*. 2017;13(1):42-59.
- Amir F Dawood, Abd AL- Rahman K and Marwa I. Mubarak. Study eosin dye adsorption on the surface waste of molasses dates production. *Diyala*

- Journal for Pure Sciences. 2017; 13(1):22-41.
10. Chia CH, Razali NF, Sajab MS, Zakaria S, Huang NM and Lim HN. Methylene blue adsorption on graphene oxide. *Sains Malaysiana*. 2013;42(6):819-826.
 11. Shahabuddin S, Sarih NM, Afzal Kamboh M, Rashidi Nodeh H and Mohamad S. Synthesis of Polyaniline-Coated Graphene Oxide@ SrTiO₃ Nanocube Nanocomposites for Enhanced Removal of Carcinogenic Dyes from Aqueous Solution. *Polymers*. 2016;8(9):305.
 12. Ahmed MJ and Theydan SK. Adsorptive removal of p-nitrophenol on microporous activated carbon by FeCl₃ activation: equilibrium and kinetics studies. *Desalination and Water Treatment*. 2015;55(2):522-531.
 13. Smaranda C, Gavrilescu M and Bulgariu D. Studies on sorption of Congo red from aqueous solution onto soil. *International Journal of Environmental Research*. 2011;5(1):177-188.
 14. Phiw dang K, Suphankij S, Mekprasart W and Pecharapa W. Synthesis of CuO nanoparticles by precipitation method using different precursors. *Energy Procedia*. 2013;34:740-745.
 15. Jing L, Xu Z, Shang J, Sun X, Cai W and Guo H. The preparation and characterization of ZnO ultrafine particles. *Materials Science and Engineering: A*. 2002;332(1):356-361.
 16. Hassan KH, Al-Bayati THM and Abbas ZMA. study and characterization of copper oxide nanoparticles prepared by chemical method using X-ray diffraction and scanning Electron Microscope. *American Journal of Scientific Research*. 2012;77:49-53.
 17. Zhou L, Wang Y, Zou, H, Liang X, Zeng K, Liu Z and Adesina AA. Biosorption characteristics of uranium (VI) and thorium (IV) ions from aqueous solution using CaCl₂-modified Giant Kelp biomass. *Journal of Radioanalytical and Nuclear Chemistry*. 2016; 307(1):635-644.
 18. Smaranda C, Gavrilescu M and Bulgariu D. Studies on sorption of Congo red from aqueous solution onto soil. *International Journal of Environmental Research*. 2011;5(1):177-188.
 19. Ho YS and McKay G. Pseudo-second order model for sorption processes. *Process Biochemistry*. 1999;34:451-465.
 20. Chook SW, Chia CH, Zakaria S, Ayob MK, Huang NM, Neoh HM and Jamal R. Antibacterial hybrid cellulose-graphene oxide nanocomposite immobilized with silver nanoparticles. *RSC Advances*. 2015; 5(33):26263-26268.
 21. Langmuir I. The adsorption of gases on plane surfaces of glass, mica and platinum. *Journal of the American Chemical society*. 1918;40(9):1361-1403.
 22. Ma J, Guo H, Lei M, Zhou X, Li F, Yu T and Wu Y. Arsenic adsorption and its fractions on aquifer sediment: effect of pH, arsenic species, and iron/manganese minerals. *Water, Air, & Soil Pollution*. 2015; 226(8): 260.
 23. Chou TC and Talalay P. Quantitative analysis of dose-effect relationships: the combined effects of multiple drugs or enzyme inhibitors. *Advances in enzyme regulation*. 1984;22:27-55.
 24. Kalyani R and Gurunathan K. PTh-rGO-TiO₂ nanocomposite for photocatalytic hydrogen production and dye degradation. *Journal of Photochemistry and Photobiology A: Chemistry*. 2016; 329:105-112.
 25. De Carvalho TE, Fungaro DA, Magdalena CP and Cunico P. Adsorption of indigo carmine from aqueous solution using coal fly ash and zeolite from fly ash. *Journal of Radioanalytical and Nuclear Chemistry*. 2011;289(2):617-626.
 26. San Miguel G, Fowler GD and Sollars CJ. A study of the characteristics of activated carbons produced by steam and carbon dioxide activation of waste tyre rubber. *Carbon*. 2003;41(5): 1009-1016.
 27. Özcan AS, Erdem B and Özcan A. Adsorption of Acid Blue 193 from aqueous solutions onto Na-bentonite and DTMA-bentonite. *Journal of Colloid and Interface Science*. 2004;280(1): 44-54.
 28. Bhat A, Megeri GB, Thomas C, Bhargava H, Jeevitha C, Chandrashekar S and Madhu G. M. Adsorption and optimization studies of lead from aqueous solution using γ-Alumina. *Journal of Environmental Chemical Engineering*. 2015;3(1):30-39.

29. Rodríguez-Martínez CE, González-Acevedo ZI, Olguín MT and Frías-Palos H. Adsorption and desorption of selenium by two non-living biomasses of aquatic weeds at dynamic conditions. *Clean Technologies and Environmental Policy*. 2016;18(1):33-44.
30. Lakshmi UR, Srivastava VC, Mall ID and Lataye DH. Rice husk ash as an effective adsorbent: Evaluation of adsorptive characteristics for Indigo Carmine dye. *Journal of Environmental Management*. 2009;90(2):710-720.